THE JOURNAL OF BIOLOGICAL CHEMISTRY VOL. 285, NO. 44, pp. 34155–34167, October 29, 2010

Chondroitin Sulfate Synthase-2/Chondroitin Polymerizing Factor Has Two Variants with Distinct Function*[S]

Received for publication, January 31, 2010, and in revised form, July 26, 2010 Published, JBC Papers in Press, August 21, 2010, DOI 10.1074/jbc.M110.109553

Hiroyasu Ogawa[‡§], Masafumi Shionyu[¶], Nobuo Sugiura[‡], Sonoko Hatano[‡], Naoko Nagai[‡], Yukihiko Kubota[‖], Kiyoji Nishiwaki[‖], Takashi Sato[**], Masanori Gotoh[**], Hisashi Narimatsu[**], Katsuji Shimizu[§], Koji Kimata[‡‡], and Hideto Watanabe[‡1]

From the [‡]Institute for Molecular Science of Medicine, Aichi Medical University, Nagakute, Aichi 480-1195, the [¶]Department of Bioscience, Faculty of Bioscience, Nagahama Institute of Bio-Science and Technology, Nagahama 526-0829, the [‖]School of Science and Technology, Kwansei Gakuin University, Sanda 669-1337, the [**]Research Center for Medical Glycoscience, Advanced Industrial Science and Technology, Tsukuba 305-8568, the [§]Department of Orthopaedic Surgery, Gifu University, Graduate School of Medicine, Gifu 501-1194, and the [‡‡]Research Complex for Medicine Frontiers, Aichi Medical University, Nagakute, Aichi 480-1195, Japan

Chondroitin sulfate (CS) is a polysaccharide consisting of repeating disaccharide units of *N*-acetyl-D-galactosamine and D-glucuronic acid residues, modified with sulfated residues at various positions. To date six glycosyltransferases for chondroitin synthesis have been identified, and the complex of chondroitin sulfate synthase-1 (CSS1)/chondroitin synthase-1 (ChSy-1) and chondroitin sulfate synthase-2 (CSS2)/chondroitin polymerizing factor is assumed to play a major role in CS biosynthesis. We found an alternative splice variant of mouse CSS2 in a data base that lacks the N-terminal transmembrane domain, contrasting to the original CSS2. Here, we investigated the roles of CSS2 variants. Both the original enzyme and the splice variant, designated CSS2A and CSS2B, respectively, were expressed at different levels and ratios in tissues. Western blot analysis of cultured mouse embryonic fibroblasts confirmed that both enzymes were actually synthesized as proteins and were localized in both the endoplasmic reticulum and the Golgi apparatus. Pulldown assays revealed that either of CSS2A, CSS2B, and CSS1/ChSy-1 heterogeneously and homogeneously interacts with each other, suggesting that they form a complex of multimers. *In vitro* glycosyltransferase assays demonstrated a reduced glucuronyltransferase activity in CSS2B and no polymerizing activity in CSS2B co-expressed with CSS1, in contrast to CSS2A co-expressed with CSS1. Radiolabeling analysis of cultured COS-7 cells overexpressing each variant revealed that, whereas CSS2A facilitated CS biosynthesis, CSS2B inhibited it. Molecular modeling of CSS2A and CSS2B provided support for their properties. These findings, implicating regulation of CS chain polymerization by CSS2 variants, provide insight in elucidating the mechanisms of CS biosynthesis.

Chondroitin sulfate (CS)[2] is a linear polysaccharide consisting of repeating disaccharide units of *N*-acetyl-D-galactosamine (GalNAc) and D-glucuronic acid (GlcUA) residues, modified with sulfated residues at various positions (1–4). CS chains exhibit structural diversity in chain length and sulfation patterns, providing specific biological functions in cell adhesion, morphogenesis, neural network formation, and cell division (5–10).

CS biosynthesis is initiated by transfer of GalNAc to the linkage region of a GlcAβ1–3Galβ1–3Galβ1–4Xyl tetrasaccharide primer that is attached to a serine residue of a core protein. Then chain polymerization takes place by the alternative addition of GalNAc and GlcUA residues. The enzymatic activities that catalyze CS initiation and polymerization processes are designated glycosyltransferase-I and -II activities, respectively (4). To date six glycosyltransferases for chondroitin synthesis have been identified: chondroitin sulfate synthase-1 (CSS1)/chondroitin synthase-1 (ChSy-1), chondroitin sulfate synthase-2 (CSS2)/chondroitin polymerizing factor (ChPF), chondroitin sulfate synthase-3 (CSS3)/chondroitin synthase-2 (ChSy-2), chondroitin sulfate glucuronyltransferase/chondroitin synthase-3 (ChSy-3), and chondroitin *N*-acetylgalactosaminyltransferase-1 and -2 (11–17). All contain an N-terminal transmembrane domain; thus, they are type II-membrane proteins. CSS1, CSS2, and CSS3 contain two glycosyltransferase domains, β-3 domain at the N-terminal region and β-4 domain at the C-terminal region and exhibit dual enzymatic activities of *N*-acetylgalactosaminyltransferase-II (GalNAcT-II) and glucuronyltransferase-II (GlcAT-II). Chondroitin sulfate glucuronyltransferase, similarly containing two glycosyltransferase domains, shows only GlcAT-I activity (12), although another report also indicated GalNAcT activity (15). Chondroitin sulfate *N*-acetylgalactosaminyltransferase-1 and -2 exhibit both GalNAcT-I and GalNAcT-II activities respon-

* This work was supported by a grant-in-aid for Scientific Research B (to H. W., and M. S.), by Japan Society for the Promotion of Science KAKENHI Grant 18370061, and by the New Energy and Industrial Technology Development Organization.

[S] The on-line version of this article (available at http://www.jbc.org) contains supplemental Figs. S1 and S2.

[1] To whom correspondence should be addressed: Karimata 21, Yazako, Nagakute, Aichi-gun, Aichi 480-1195, Japan. Tel.: 81-561-62-3311 (ext. 2088); Fax: 81-561-63-3532; E-mail: wannabee@aichi-med-u.ac.jp.

[2] The abbreviations used are: CS, chondroitin sulfate; CH, chondroitin; CSA-8, octasaccharide of chondroitin sulfate A; CSC-8 and -9, octasaccharide and nanosaccharide of chondroitin sulfate C; CSS, chondroitin sulfate synthase; ChSy, chondroitin synthase-1; ER, endoplasmic reticulum; GalNAcT, *N*-acetylgalactosaminyltransferase; GlcUA, D-glucuronic acid; GlcAT, glucuronyltransferase; GAG, glycosaminoglycan; MEF, mouse embryonic fibroblast; ChPF, chondroitin polymerizing factor; Mfng, mouse fringe.

sible for chain initiation and polymerization, respectively. Although CSS1, CSS2, and CSS3 show both GlcAT and GalNAcT activities, none of these enzymes show chain polymerization individually. Characterization of these enzymes has revealed that samples obtained from cells co-expressed with a combination of two dual enzymes has polymerizing activity, but a mixture of the two does not (18). These observations suggest that a complex of two glycosyltransferases is the core machinery for CS polymerization and that it can only be formed in the cell.

Because coexpression of dual enzymes has been shown necessary for CS chain polymerization (15, 18), the other two enzymes may be redundant, or different pairs may exert a distinct function. In addition, co-expression of different pairs causes differences in chain length polymerized (18). However, the mechanism of how the partnership causes the chain length remains to be understood. As various factors including sulfation levels and patterns have been shown to affect CS chain length (19, 20), the differences in CS chain length observed by *in vitro* assay systems may not recapitulate *in vivo* CS biosynthesis.

CSS1, CSS2, CSS3, and chondroitin sulfate glucuronyltransferase are expressed ubiquitously rather than in a tissue-specific manner, although there are some exceptions. Among these enzymes, CSS1 exhibits the highest expression level and GlcAT and GalNAcT activities followed by CSS2 (13, 14). In contrast, the expression levels of CSS3 are considerably low (21). These observations strongly suggest that the complex of CSS1 and CSS2 plays the major role in CS chain polymerization *in vivo*. However, the molecular mechanisms of complex formation and its CS chain polymerization have not been elucidated.

Fortuitously, we found an alternative splice variant of mouse CSS2 in the gene data base at the National Center for Biotechnology Information (National Institutes of Health, Bethesda, MD). The splice variant (GenBank^{TM} accession number NM_001001565) is supposed to lack the transmembrane, contrasting to the original/authentic CSS2 (GenBank^{TM} accession number NM_001001566). In this study we investigated the roles of CSS2 by comparing the original enzyme CSS2A with the splice variant CSS2B. Both CSS2A and CSS2B were indeed expressed in various tissues and were localized in both the endoplasmic reticulum (ER) and the Golgi apparatus. Pulldown assays revealed homogenous and heterogeneous interaction among CSS2A, CSS2B, and CSS1/ChSy-1, suggesting that they form a complex of multimers. A series of *in vitro* glycosyltransferase assays demonstrated a reduced GlcAT activity in CSS2B that was supported by molecular modeling. CSS2B co-expressed with CSS1 exhibited no polymerizing activity, in contrast to CSS2A co-expressed with CSS1. Moreover, analysis of CS biosynthesis revealed inhibition by CSS2B. These findings, implicating regulation of CS chain polymerization by CSS2 variants, provide insight into the mechanisms of CS biosynthesis by CSS1 and CSS2.

EXPERIMENTAL PROCEDURES

Materials—Uridine diphosphate (UDP)-[^{3}H]GalNAc (7.0 Ci/mmol), [^{35}S]sulfate (38.8–59.2 TBq/mmol), and sodium [^{3}H]borohydride (2.96–3.7 TBq/mmol) were purchased from PerkinElmer Life Sciences, and UDP-[^{14}C]GlcUA (313 mCi/mmol) was from ICN Biomedicals (Irvine, CA). Chondroitinase ABC and chondroitin (a chemically desulfated derivative of whale cartilage chondroitin sulfate A) were from Seikagaku Biobusiness (Tokyo, Japan). Superdex^{TM} peptide HR10/30, Superose 6^{TM} HR 10/30, and Superose 12^{TM} HR 10/30 columns were purchased from Amersham Biosciences.

Quantitative Real Time RT-PCR—mRNA was isolated from the rib cage and brain of C57/BL6 newborn mice and mouse embryonic fibroblasts (MEFs) grown on a 100 mm-culture dish using Micro-FastTrack^{TM} 2.0 mRNA Isolation kit (Invitrogen) according to the manufacturer's instructions. MEFs were derived from decapitated E14.5 embryos. Then cDNA was synthesized from the mRNA using SuperScript^{TM} First-Strand Synthesis System for RT-PCR (Invitrogen) according to the manufacturer's instructions. Real time PCR was performed using the cDNA, TaqMan probes, and primers specific for individual CSS2 variants and Applied Biosystems ABI Prism 7700 sequence detection system (TaqMan). TaqMan® Probes (Applied Biosystems) and primers were: 5′-6-carboxyfluorescein-TAGACCCCACCTCGGGGGCGGGGCC-6-carboxytetramethylrhodamine (TAMRA)-3′, 5′-TTCGTCCCTCTCCGCTAGCTGACG-3′, and 5′-AAGGCGGCCGCTGTCCGACGTGTC-3′ for CSS2A; 5′-tetrachloro-6-carboxy-fluorescein-(TET)-ATTGATGTCTCTGCCCACGCATTGAAGT-TAMRA-3′, 5′-CGTCAGATGGGTTTCAAGGGCCAC-3′, and 5′-CCGAGTTCTTCCTAAGGTAGAAGG-3′ for CSS2B. The reaction was performed in triplicate in 96-well optical plates using 5 ng of cDNA, 25 μl of TaqMan® Universal PCR Mastermix (Applied Biosystems), 100 nM probe, 100 nM concentrations of each primer in a final volume of 50 μl. Thermocycling conditions comprised an initial holding step at 50 °C for 2 min, 95 °C for 10 min, and 50 cycles of 95 °C for 15 s and 60 °C for 60 s. A standard curve for each gene was generated using its expression plasmid constructed as below. The copy numbers of each variant present in the tissues were determined by comparison with the appropriate standard curve. To standardize mRNA levels, TaqMan® Rodent GAPDH Control Reagents VIC^{TM} (Applied Biosystems) was used as the internal control.

Production of an Anti-CSS2 Antibody—An antiserum against a specific synthetic peptide AELERRFPGARVPWL (amino acid residues 570–584 of CSS2A and 408–422 of CSS2B) with N-terminal cysteine was raised in rabbit (Operon Biotechnology, Tokyo, Japan). The polyclonal anti-CSS2 antibody was affinity-purified from the antiserum using maleimide-Sepharose conjugated with the antigenic peptide.

Immunoprecipitation of Endogenous CSS2 Variants—MEFs derived as above were cultured in Dulbecco's modified Eagle's medium (DMEM, Sigma) containing 10% fetal bovine serum (FBS), penicillin, and streptomycin, and the cells at passage 4 were grown up to the confluence on twenty 15-cm culture dishes. After treatment with 0.05% trypsin, cells were collected using DMEM containing 10% FBS and washed twice in ice-cold phosphate-buffered saline (PBS). Cell pellets were suspended in 40 ml of cell lysis buffer (10 mM Tris-HCl, pH 7.4, 1.5 mM EDTA, 140 mM NaCl, 1% Triton X-100, 25 mM NaF, with freshly added proteinase inhibitor mixture). The lysate was incubated for 1 h at 4 °C in a rotation shaker and clarified by centrifugation (14,000 rpm for 30 min at 4 °C).

The supernatant of the lysate was first incubated with 30 μl of Protein G-Sepharose™ 4 Fast Flow (GE Healthcare) for pre-clearing for 2 h at 4 °C in a rotation shaker and then incubated overnight at 4 °C in a rotation shaker with 20 μg of anti-CSS2 antibody pre-bound to 30 μl of Protein G-Sepharose ™ 4 Fast Flow. As a control for anti-CSS2 antibody in immunoprecipitation, the same amount of normal rabbit IgG was used. The beads were recovered by centrifugation and washed five times with PBS and then subjected to Western blot analysis.

Western Blot Analysis—Proteins were separated by 10% SDS-PAGE and transferred to a polyvinylidene difluoride membrane according to standard procedures. After blocking for 1 h in TBS (20 mM Tris-HCl pH 7.4, 150 mM NaCl) containing 5% skim milk and 0.1% Tween 20 at room temperature, the membrane was incubated with anti-CSS2 antibodies for 1 h at room temperature. After washing with TBS for 10 min 3 times, the membrane was incubated with goat anti-rabbit antibodies conjugated with horseradish peroxidase (Cappel) for 1 h at room temperature. After washing with TBS as above, proteins bound to the antibodies were visualized with SuperSignal® West Femto Maximum Sensitivity Substrate (Thermo Scientific) according to the manufacturer's instruction.

Construction of Expression Plasmids of CSS2A Variants and CSS1—Expression plasmids for soluble forms of CSS2A, CSS2B, and CSS1 were constructed as follows. The cDNA fragments of CSS2A, CSS2B, and CSS1 were amplified by PCR from the I.M.A.G.E cDNA clones (Invitrogen) and cDNA from a C57/Bl6 mouse, as described for "Quantitative Real Time RT-PCR," as templates, respectively. These cDNA fragments lacked the N-terminal transmembrane domain (11). Primers used were: 5′-GCGGATATCACCCGGAGACTCTGAGCTGC-CGC-3′ and 5′-ATATCTAGAGGCTCTAGGGCATCTGT-CTC-3′ for CSS2A; 5′-ATAGATATCGGTGGTGGCACTG-GGCGAAG-3′ and 5′-ATATCTAGAGGCTCTAGGGCAT-CTGTCTC-3′ for CSS2B; 5′-ATAGATATCCGTGCTGGCC-TCGCGGCTCG-3′ and 5′-ATATCTAGATGTTCAGCAAG-GTGTGTTCGAAGG-3′ for CSS1/ChSy-1 containing EcoRV sites (forward primers, GATATC) and XbaI sites (reverse primers, TCTAGA) (underlined), respectively. The PCR was carried out using *KOD*-Plus DNA polymerase (Toyobo Biochemicals) with a program of 35 cycles of 98 °C for 10 s, 75 °C for 30 s, and 68 °C for 5 min. The amplified fragments were inserted using EcoRV and XbaI sites of the pFLAG-CMV3 vector (Sigma), which contains a secretion signal of preprotrypsin and a FLAG tag.

Expression plasmids for CSS2 variants that initiate at the start codon were constructed as follows. The cDNA fragments encoding CSS2A and CSS2B were amplified as described above using primers: 5′-TAATTGATATCGCTGCGGCCCGCG-3′ and 5′-ACGTCTAGAGGCAAGCTGGGTGCG-3′ for CSS2A and 5′-AACAGAATTCCCTGACCGGTGCGAG-3′ and 5′-ACGTCTAGAGGCAAGCTGGGTGCG-3′ for CSS2B, containing EcoRI or EcoRV and containing XbaI sites (underlined) for forward and reverse primers, respectively. PCR was carried out using *KOD*-Plus DNA polymerase (TOYOBO) with a program of 35 cycles at 98 °C for 10 s, 60 °C for 30 s, and 68 °C for 180 s. The amplified fragments were inserted to p3×FLAG-CMV14 vectors (Sigma) using the EcoRV or EcoRI and XbaI sites, which contains a 3×FLAG tag sequence at the C terminus of the insert.

Expression plasmids for Myc-tagged CSS1 and the CSS2 variants were constructed as follows. The cDNA fragments encoding CSS2A, CSS2B, and CSS1 were amplified as described above using primers: 5′-ATAGATATCGGGCTTGAGCTCC-TACCTCTGC-3′ and 5′-ATATGCGGCCGCTGTTCCCCT-GTTC-3′ for CSS2A; 5′-AACAGAATTCCCTGACCGGTGC-GAG-3′ and 5′-ATATGCGGCCGCTGTTCCCCTGTTC-3′ for CSS2B; 5′-AGGATATCGCATGGTCCCCTCTTAAAG-GCG-3′ and 5′-AAATCTAGACCGTGGCTGCCACCTTT-GCTG-3′ for CSS1, containing EcoRI or EcoRV and containing XbaI or NotI sites (underlined), respectively. The PCR products were inserted into the pEF/*Myc*-His vector (Invitrogen) using appropriate restriction sites. DNA sequencing using an ABI PRISM® 3130 Genetic Analyzer (Applied Biosystems) confirmed the amplified cDNA in these expression plasmids.

Expression of Soluble Forms of CSS1 and CSS2 Variants and Enzyme Assays—COS-7 cells grown in a 100-mm dish were transfected with the expression plasmid (6 μg) using FuGENE™ 6 (Roche Applied Science) according to the manufacturer's instructions. For co-expression experiments, two expression plasmids (3.0 μg each) were used. Three days after the transfection, a proteinase inhibitor mixture was added to 10 ml of the conditioned medium, and the medium was collected and incubated with 20 μl of anti-FLAG M2-agarose gel (Sigma) overnight at 4 °C. The beads were recovered by centrifugation, washed with TBS containing 0.1% Tween 20, and then resuspended in the assay buffer below. The amount of recombinant protein recovered was determined as follows. Western blot with known amounts at 5 points of FLAG-tagged KfiA (molecular mass = 29 kDa) (22) was performed, and the band density at a linear correlation was obtained. The band density of FLAG-tagged enzyme was measured by densitometry, and the molecular number of the enzyme (mol) was determined using the standard curve. The amount of the enzyme was calculated with the known molecular weight of the enzymes. A Western blot confirmed that equal amounts of CSS2A and CSS2B were on the gel beads. Assays for glycosyltransferase and polymerizing activity were carried out using UDP-[^{14}C]GlcUA, UDP-[^{3}H]GalNAc, and UDP-GalNAc as donors and oligosaccharides as acceptors, as described previously (11, 12). Oligosaccharides including octasaccharide of chondroitin (CH-8), octasaccharides of chondroitin sulfate A (CSA-8), octa- and nanosaccharides of chondroitin sulfate C (CSC-8 and CSC-9), and GlcUAβ1–3Galβ1–3Galβ1–4Xylβ1-*O*-methoxyphenyl were prepared. The reaction mixture for GalNAcT-II assay contained 10 μl of the gel slurry, 0.32 nmol of UDP-[^{3}H]-GalNAc (7.0 Ci/mmol), 1 nmol of CSC-8, 50 mM MES, pH 6.2, and 10 mM $MnCl_2$ in a total volume of 30 μl. The reaction mixture for GlcAT-II assay contained 10 μl of the gel slurry, 0.33 nmol of UDP-[^{14}C]GlcUA (313 mCi/mmol), 1 nmol of CSC-9, 50 mM MES, pH 6.2, and 10 mM $MnCl_2$ in a total volume of 30 μl. The reaction mixture for initiating and polymerizing activities contained 10 μl of the gel slurry, 0.33 nmol of UDP-[^{14}C]GlcUA, 33 nmol of UDP- GlcUA, 33 nmol of UDP-GalNAc as donors, and either of 1 nmol of CSA-8, CSC-8, CH-8, and GlcUAβ1–3Galβ1–3Galβ1–4Xylβ1-*O*-methoxy-

phenyl as acceptor substrates, 50 mM MES, pH 6.2, and 10 mM $MnCl_2$ in a total volume of 30 μl. The reaction mixture was incubated at 37 °C for 1 h with mixing, and the reaction was stopped by boiling for 5 min, and then the radiolabeled products were applied to Superdex™ peptide HR10/30 column equilibrated with 0.2 M NaCl followed by scintillation counting of each fraction, as described previously (11, 12).

Assessment of Secretion of CSS2 Variants—COS-7 cells grown in 6-well plates were transfected with the expression plasmid (1 μg) for the full-length enzyme attached with FLAG tag at the C terminus using FuGENE 6 (Roche Applied Science). After 48 h, the FLAG-tagged enzyme in cell lysates and medium was absorbed with 10 μl of anti-FLAG M2-agarose gel. The beads recovered by centrifugation were washed with TBS containing 0.1% Tween 20 and subjected to Western blot analysis as described above. The density of bands was measured to compare the expression levels of the CSS2 variants in cell lysates and medium using a densitometer, Multi Gauge Version 3 (FUJIFILM).

Immunocytochemical Analysis of CSS2 Variants—For assessment of intracellular localizations of CSS2 variants, the expression plasmid (0.6 μg) was transfected into BALB 3T3 cells grown in wells of Lab-Tek® II Chamber Slide™ Systems (Two-well, Nalge Nunc International) using FuGENE 6 (Roche Applied Science) according to the manufacturer's instructions. After 48 h, the cells were washed with PBS and fixed with cold methanol for 20 min and cold acetone for 1 min and then double-immunostained as follows. For detection of FLAG-tagged protein, the mouse monoclonal anti-FLAG M2 antibody and Alexa Fluor® 488 goat anti-mouse IgG (Invitrogen) were used as the primary and secondary antibodies, respectively. To assess the ER and the Golgi apparatus, a rabbit polyclonal anti-PDI antibody (Stressgen Biotechnologies) and a rabbit monoclonal anti-Golgi Matrix Protein (GM130) antibody (Epitomics) were used as the primary antibodies, respectively, and Alexa Fluor® 594 goat anti-rabbit IgG (Invitrogen) was used as the secondary antibody. The cells were observed using a fluorescence microscope, BZ-8000 (Keyence).

Pulldown Assays—Various combinations of FLAG- and Myc-tagged CSS2A, CSS2B, and CSS1 expression plasmids were co-transfected in COS-7 cells grown in 6-well plates as described above. After 48 h, immunoprecipitation was performed using anti-FLAG M2-agarose gel as described above, and the gel slurry was subjected to Western blot analysis. For detection of Myc-tagged proteins, mouse monoclonal anti-Myc antibodies (Nacalai Tesque) and goat anti-mouse antibodies conjugated with horseradish peroxidase (Cappel) were used as the first and secondary antibodies, respectively.

Size Exclusion Chromatography of a Multimolecular Complex of CSS—Various combinations of FLAG- and Myc-tagged CSS2A, CSS2B, and CSS1 expression plasmids were co-transfected in COS-7 cells grown in 6-well plates as described above. After 48 h, cell were suspended in 200 ml of cell lysis buffer (50 mM Tris-HCl, pH 6.8, 1.5 mM EDTA, 150 mM NaCl, 1% Triton X-100, with freshly added proteinase inhibitor mixture). The lysate was incubated for 1 h at 4 °C in a rotation shaker and clarified by centrifugation (14,000 rpm for 30 min at 4 °C). The supernatant was applied to a Superose 6 column (Amersham Biosciences) equilibrated in 50 mM Tris-HCl, pH 6.8, 0.15 M NaCl, 0.1% CHAPS. Each fraction (1 ml) was precipitated using 10% trichloroacetic acid. The pellet was dissolved with distilled water and subjected to Western blotting analysis as described above.

Analysis of CS Biosynthesis Using [^{35}S]Sulfate—COS-7 cells in 6-well plates were transfected with the expression plasmids of CSS2 variants used for immunostaining above. After 24 h the medium was replaced with Nutrient Mixture F-12 Ham's medium (Sigma) containing [^{35}S]sulfate (100 μCi/ml). Twenty-four hours after the medium replacement, the cells were washed with PBS 3 times, and glycosaminoglycans (GAGs) were isolated, as previously reported (23). Briefly, the cells were treated with 0.2 M NaOH for 16 h at room temperature, neutralized by the addition of 4 M acetate, treated with DNase and RNase for 2 h at 37 °C, and digested with 1 mg/ml proteinase K in 50 mM Tris-HCl, pH 8.0, for 2 h at 55 °C. After centrifugation for 10 min at 10,000 × *g*, the sample was applied to a DEAE-Sephacel (Amersham Biosciences) column equilibrated with 50 mM Tris-HCl, pH 7.5. After washing with 10 column volumes of 50 mM Tris-HCl, pH 7.5, 0.2 M NaCl, GAG-rich fractions were eluted with 3 column volumes of 50 mM Tris-HCl, pH 7.5, 2 M NaCl. The eluate was precipitated by an addition of 3 volumes of 95% ethanol containing 1.3% potassium acetate, and the precipitate was dissolved in 100 μl of distilled water. The sample was treated with a mixture of 10 microunits/ml heparitinase I (Seikagaku), 5 microunits/ml heparitinase II (Seikagaku), and 10 microunits/ml heparinase (Seikagaku) in 50 mM Tris-HCl, pH 7.2, 1 mM $CaCl_2$ for 2 h at 37 °C and applied to an Ultrafree®-MC Filter Units (Millipore), and the sample remaining in the filter cup was recovered by 60 μl of distilled water. To evaluate the total amount of [^{35}S]sulfate incorporation, a portion (30 μl) of the sample was measured by scintillation counting. To examine the chain length, the other sample was applied to a Superose 6 column equilibrated in 0.2 M CH_3COONH_4 followed by scintillation counting of each fraction, as described previously (23). To confirm that glycosaminoglycan-rich fractions contained CS, in a separate experiment a portion (30 μl) of the sample treated with chondroitinase ABC was similarly subjected to gel filtration followed by scintillation counting. Radioactivity was expressed per mg on cell protein, which was quantified after the NaOH treatment using Micro BCA™ protein assay kit (Pierce) according to the manufacturer's instructions.

Analysis of CS Chain Length in Tissue—GAG was isolated from the brain of mice and treated with the heparitinase mixture as described under "Analysis of CS Biosynthesis Using [^{35}S]Sulfate." An aliquot of the extracted GAGs was labeled with sodium [^{3}H]borohydride. Briefly, 10 μl of sample source was reacted with 8.4 pmol of sodium [^{3}H]borohydride (12 nCi/pmol) for 3 h at room temperature, treated with 2 μl of 2 M CH_3COOH, and neutralized with 2 μl of 2 M NaOH. After the removal of free sodium [^{3}H]borohydride by precipitation using 3 volumes of 95% ethanol containing 1.3% potassium acetate, the labeled sample was applied to a Superose 6 column under the same conditions as above.

Homology Modeling of the N-terminal Domain of CSS2 Variants—By homology modeling, we estimated the three-dimensional structure of the N-terminal domain of CSS2 variants

(N-CSS2A and N-CSS2B), as follows. Because there was no significant sequence similarity to other glycosyltransferases (in which three-dimensional structures are known), obtained by BLAST search, we searched for a template structure using four protein fold recognition programs, including FUGUE (35), FORTE (36), GenThreader (37), and Phyre (24). All the methods showed the catalytic domain (25) (PDB code 2j0a) of murine Manic Fringe (Mfng) had the best score with N-CSS2A. As only Phyre aligned disordered regions of Mfng to N-CSS2A properly, we performed homology modeling based on the alignment obtained by Phyre using the three-dimensional structure of Mfng as a template. To build the model, we used two programs, the molecular operating environment (MOE, Chemical Computer Group, Inc.) and Discovery Studio 2.5 (DS, Accelrys Inc.). For the homology modeling using MOE, the default settings except for AMBER99 force field parameters were used. For the homology modeling using DS, 10 models were built using default parameters. Ofthem, a model structure showing the lowest probability density function total energy and the highest discrete optimized protein energy structure, was chosen. The candidate structures obtained by MOE and DS were evaluated using Profiles three-dimension and the model structure with the highest Verify Score chosen as the model structure of N-CSS2A. Similar to N-CSS2A, Phyre showed Mfng had the best score with N-CSS2B. Based on the alignment of N-CSS2A and Mfng obtained by Phyre, we removed the segment of amino acid residues 1–162, which is a missing region in N-CSS2B. The putative β-strand region at the N terminus of N-CSS2B was aligned to the first β-strand of Mfng, ^{58}IAVKTT^{63}, manually. Then we built a model structure of N-CSS2B by MOE and DS using Mfng (PDB code 2j0a) as template. In the N-CSS2B modeling, the same parameters for N-CSS2A modeling described above were used.

Next, using the three-dimensional structure of the complex of Mfng and UDP-Mn^{2+} (PDB code 2j0b), we estimated the model structure of the complex of N-CSS2A and UDP-Mn^{2+}. We superposed the model structure of N-CSS2A onto the Mfng-UDP-Mn^{2+} complex and then removed the Mfng structure. Then, using the LigX program of MOE, we optimized the conformation of amino acid residues surrounding the UDP-Mn^{2+}. We defined it as the model of N-CSS2A-UDP-Mn^{2+} complex. Similarly, we estimated the model of N-CSS2B-UDP-Mn^{2+} complex. Subsequently, we identified the amino acid residues that interact with UDP-Mn^{2+} in the Mfng-UDP-Mn^{2+} complex. The interacting residues were defined as the amino acid residues whose accessible surface area in the Mfng-UDP-Mn^{2+} complex structure was larger than 10 Å^2 regardless of the presence of UDP-Mn^{2+}. By the same criteria, we predicted the interacting residues with UDP-Mn^{2+} of the N-CSS2A/N-CSS2B from the complex model structures.

RESULTS

Comparison of Genomic Organizations and Amino Acid Sequences of CSS2 Variants—The genomic organization and amino acid sequences of two variants of mouse CSS2/ChPF are shown in Fig. 1. The gene of CSS2, initially reported and here designated as CSS2A, comprises four exons (Fig. 1*A*) containing two in-frame ATGs (ATG-1 and ATG-2). In contrast, the gene of an alternative splice variant designated CSS2B has an additional exon, designated exon 1′, between exon 1 and 2 of CSS2A gene. In addition, exon 1 of CSS2B lacks the first 94 nucleotides in that of CSS2A, indicating a difference in transcriptional start sites between the two variants. The data base shows that the translation of CSS2B initiates at ATG-2, whereas that of CSS2A does so at ATG-1. The resulting CSS2B is supposed to lack an N-terminal region of 162 amino acid residues of CSS2A. As this region contains the transmembrane domain, the CSS2B protein is supposed to lack an anchor to the membrane. In addition, without an *N*-glycosylation site and a cysteine residue, CSS2B may be structurally unstable compared with CSS2A. Two (putative) D*X*D motifs, key sequences for divalent cation binding, at the N-terminal and C-terminal regions of CSS2A, are found in those of CSS2B (Fig. 1*B*, *half-boxed*). Both the β3-glycosyltransferase and β4-glycosyltransferase motifs are also conserved (Fig. 1*B*, *boxed with dotted and solid lines*). These observations suggest that CSS2B functions as a dual glycosyltransferase similar to CSS2A.

Analysis of Transcription Levels of CSS2 Variants—Initially, we investigated whether CSS2B was transcribed in CS-synthesizing cells and tissues in mouse. Real-time RT-PCR with variant-specific primers and probes was applied to quantify the levels of each transcript of the variants. Standard curves were generated for each variant using concentration-known DNA fragments as standard, and the amplification efficiency for each of the variants was verified to be ≥0.99. The transcription levels of CSS2 variants in rib cage and brain of newborn mice and MEFs were shown as the absolute amount *versus* the glyceraldehydes-3-phosphate dehydrogenase (GAPDH) transcripts (Fig. 2*A*). The relative transcription level of CSS2B to CSS2A was 1.8, 10.0, and 16.3% in MEF, brain, and rib cage, respectively. These results indicate that CSS2B is expressed generally in CS-containing tissues and suggest tissue-specific transcriptional regulation of CSS2 variants.

CSS2 Variants Are Synthesized as Proteins—Next, we examined whether CSS2B is expressed as a protein or not. Although molecular cloning of six glycosyltransferases was performed, there has been no report showing identification of these endogenous enzymes. Thus, we generated an anti-CSS2 antibody that recognizes both variants and confirmed its specificity by Western blot analysis of FLAG-tagged CSS2 variants (supplemental Fig. S1). As Western blot analysis using samples from cartilage, brain, and cell lysates of MEFs failed to detect the endogenous CSS2, we enriched the endogenous protein by immunoprecipitation using the specific antibody. When the immunoprecipitates of the cell lysate obtained from at least 6×10^7 MEFs were subjected to Western blot analysis, both CSS2A and CSS2B were observed at an expected molecular mass of 85 and 68 kDa, respectively (Fig. 2*B*).

Glycosyltransferase Activities of CSS2 Variants—Previously, we demonstrated that human CSS2 has both GalNAcT-II and GlcAT-II activities (11), whereas another research group reported that it has little glycosyltransferase activity but attains polymerizing activity for disaccharide-repeating units of CS when co-expressed with soluble human CSS1/ChSy-1 (14). Therefore, we investigated whether mouse CSS2 variants

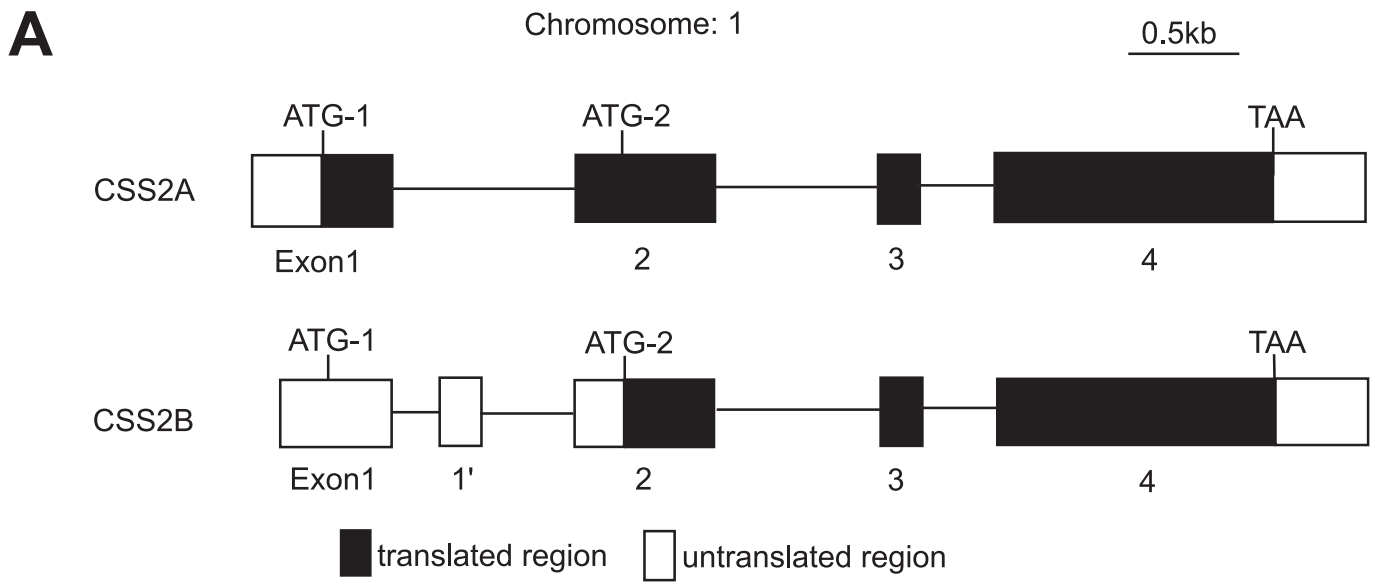

B

```
CSS2A   (1) MRASLLLSVLRPAGPVAVGISLGFTLSLLSVTWVEEPCGPGPPQPGDSELPPRGNTNAARRPNSVQPGSERERPGAGAGTGESWEPRVLPYHPAQPGQAT (100)
CSS2B       ------------------------------------------------------------------------------------------------------

CSS2A (101) KKAVRTRYISTELGIRQKLLVAVLTSQATLPTLGVAVNRTLGHRLEHVVFLTGARGRRTPSGMAVVALGEERPIGHLHLALRHLLEQHGDDFDWFFLVPD (200)
CSS2B   (1) ------------------------------------------------------------MAVVALGEERPIGHLHLALRHLLEQHGDDFDWFFLVPD (38)

CSS2A (201) ATYTEAHGLDRLAGHLSLASATHLYLGRPQDFIGGDTTPGRYCHGGFGVLLSRTLLQQLRPHLESCRNDIVSARPDEWLGRCILDATGVGCTGDHEGMHY (300)
CSS2B  (39) ATYTEAHGLDRLAGHLSLASATHLYLGRPQDFIGGDTTPGRYCHGGFGVLLSRTLLQQLRPHLESCRNDIVSARPDEWLGRCILDATGVGCTGDHEGMHY (138)

CSS2A (301) NYLELSPGEPVQEGDPRFRSALTAHPVRDPVHMYQLHKAFARAELDRTYQEIQELQWEIQNTSRLAADGERASAWPVGIPAPSRPASRFEVLRWDYFTEQ (400)
CSS2B (139) NYLELSPGEPVQEGDPRFRSALTAHPVRDPVHMYQLHKAFARAELDRTYQEIQELQWEIQNTSRLAADGERASAWPVGIPAPSRPASRFEVLRWDYFTEQ (238)

CSS2A (401) YAFSCADGSPRCPLRGADQADVADVLGTALEELNRRYQPALQLQKQQLVNGYRRFDPARGMEYTLDLQLEALTPQGGRWPLTRRVQLLRPLSRVEILPVP (500)
CSS2B (239) YAFSCADGSPRCPLRGADQADVADVLGTALEELNRRYQPALQLQKQQLVNGYRRFDPARGMEYTLDLQLEALTPQGGRWPLTRRVQLLRPLSRVEILPVP (338)

CSS2A (501) YVTEASRLTVLLPLAAAERDLASGFLEAFATAALEPGDAAALTLLLLYEPRQAQRAAHSDVFAPVKAHVAELERRFPGARVPWLSVQTAAPSPLRLMDLL (600)
CSS2B (339) YVTEASRLTVLLPLAAAERDLASGFLEAFATAALEPGDAAALTLLLLYEPRQAQRAAHSDVFAPVKAHVAELERRFPGARVPWLSVQTAAPSPLRLMDLL (438)

CSS2A (601) SKKHPLDTLFLLAGPDTVLTPDFLNRCRMHAISGWQAFFPMHFQAFHPAVAPPQGPGPPELGRDTGHFDRQAASEACFYNSDYVAARGRLVAASEQEEEL (700)
CSS2B (439) SKKHPLDTLFLLAGPDTVLTPDFLNRCRMHAISGWQAFFPMHFQAFHPAVAPPQGPGPPELGRDTGHFDRQAASEACFYNSDYVAARGRLVAASEQEEEL (538)

CSS2A (701) LESLDVYELFLRFSNLHVLRAVEPALLQRYRAQPCSARLSEDLYHRCRQSVLEGLGSRTQLAMLLFEQEQGNST (774)
CSS2B (539) LESLDVYELFLRFSNLHVLRAVEPALLQRYRAQPCSARLSEDLYHRCRQSVLEGLGSRTQLAMLLFEQEQGNST (638)
```

FIGURE 1. **Genomic structure of CSS2A and CSS2B and alignment of their amino acid sequences.** *A*, shown is the genomic structure of CSS2A and CSS2B. CSS2A has two in-frame ATGs (ATG-1 and ATG-2) in exon 1 and 2. The alternatively spliced variant CSS2B lacks the first 94 nucleotides in exon 1 of CSS2A, has an additional exon (exon 1′) of 143 nucleotides between exon 1 and 2, and shows a shift of the putative translational start site of ATG-1 to ATG-2. *B*, shown is alignment of amino acid sequences. The transmembrane domain is *underlined*. *Half-boxes above* the sequences show putative D*X*D motifs. The β3-glycosyltransferase motif is *boxed with broken line*, and the β4-glycosyltransferase motif is *boxed with solid line*. Possible *N*-glycosylation sites are indicated by *asterisks*. Cysteine residues are marked by *triangles*. CSS2B with translation initiation at ATG-2 lacks the first 162 amino acid residues of CSS2A containing a transmembrane domain.

exhibit glycosyltransferase activity or not. Soluble CSS2 variants with the FLAG tag at the N terminus were expressed in COS-7 cells, and the conditioned media were treated with anti-FLAG M2 antibody-conjugated agarose gel. Glycosyltransferase activities were determined using either CSS2A or CSS2B-bound beads as an enzyme source, CSC as acceptor substrate, and either UDP-GalNAc or UDP-GlcUA as the donor substrate under optimized conditions (11) as described under "Experimental Procedures." GalNAcT-II and GlcAT-II activities of CSS2 variants are shown in Table 1. CSS2A exhibited both GalNAcT-II and GlcAT-II activities, consistent with our previous results of human CSS2 (11). CSS2B also showed both GalNAcT-II and GlcAT-II activities, but they were 82.8 and 26.5% that of CSS2A, respectively.

Polymerizing Activity of CSS2 Variants—CSS2 was reported to be a factor critical for chondroitin polymerization (14, 18, 26)

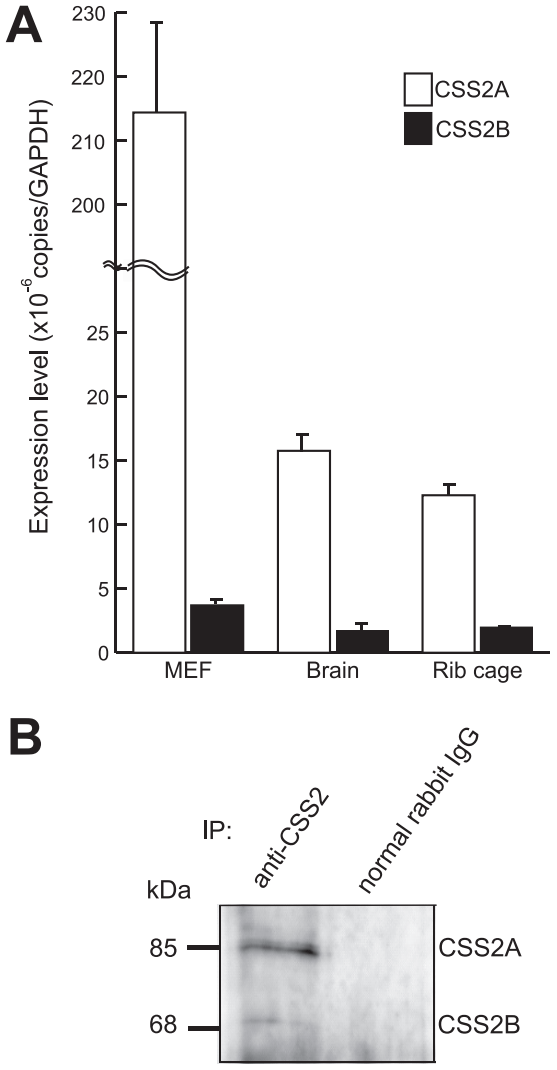

FIGURE 2. **Quantification of transcription levels by real-time RT-PCR (*A*) and identification of the CSS2 variant as protein (*B*).** *A*, standard curves for the CSS2 variants and GAPDH were generated by serial dilution of each concentration-known DNA fragment. The expression levels of the CSS2 variants were normalized with those of the GAPDH transcripts that were measured using the same cDNAs. Data are indicated as the mean ± S.D. ($n = 3$). Two identical experiments showed the same results. *B*, immunoprecipitation (*IP*) is shown of the CSS2 variants followed by a Western blot. The cell lysates obtained from at least 6×10^7 MEFs were subjected to immunoprecipitation and Western blot analysis using an anti-CSS2 antibody as described under "Experimental Procedures." Proteins bound to the antibodies were visualized with SuperSignal® West Femto Maximum Sensitivity Substrate (Thermo Scientific). As a negative control for immunoprecipitation, normal rabbit IgG was used.

TABLE 1
Comparison of GalNAcT-II and GlcAT-II activities of CSS2A and CSS2B

Protein	GalNAcT-II activity[a]	GlcAT-II activity[a]
	pmol/h/mg	*pmol/h/mg*
CSS2A	461.93 ± 9.45	143.53 ± 0.09
CSS2B	382.27 ± 29.05[b]	37.97 ± 0.20[c]
Mock	ND[d]	ND

[a] Values represent the average of three independent experiments.
[b] Significantly different compared with that of CSS2A ($p < 0.05$).
[c] Significantly different compared with that of CSS2A ($p < 0.00001$).
[d] ND, not detected (<1 pmol/mg/h).

based on the result showing that the enzyme sample obtained from cells co-expressing CSS1/ChSy-1 and CSS2 achieved polymerization, whereas either that expressing CSS1/ChSy-1

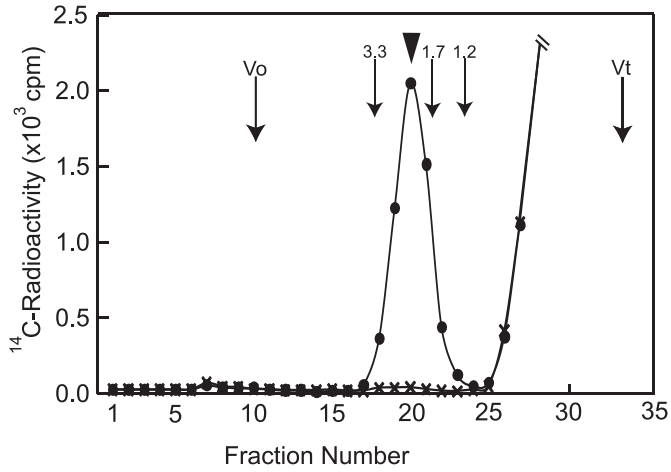

FIGURE 3. **Comparison of the chondroitin polymerization products obtained from co-expressed CSS1 and CSS2A or CSS2B.** Co-expressed CSS1 and CSS2A or co-expressed CSS1 and CSS2B were used for polymerization reactions using UDP-[^{14}C]GlcUA and UDP-GalNAc as donors and CSC-8 as an acceptor. There, the measurable products with [^{14}C]GlcUA were CSC-8 attached with two or more saccharides. The resultant products were separately applied to a Superdex peptide column, and the effluent fractions (0.5 ml each) were analyzed for radioactivity. Note that the reaction using co-expressed CSS1 and CSS2A shows a peak (●), whereas that using co-expressed CSS1 and CSS2B does not (×). *Numbered arrowheads 1.2*, *1.7*, and *3.3* indicate the eluted positions of chondroitin polysaccharides of known sizes (molecular size: 1200, 1700, and 3300, respectively).

or CSS2 did not. Using a similar assay system, we investigated whether or not CSS2 variants accomplish chondroitin polymerization. We co-expressed both CSS1 with FLAG tag and either CSS2 variant with the tag and used anti-FLAG gel slurry that bound the co-expressed proteins in the conditioned medium as the enzyme sample, as described under "Experimental Procedures." The expression levels were confirmed to be similar between CSS1 and either CSS2 variant using Western blot analysis. When CSC-8 as acceptor substrate and UDP-[^{14}C]GlcUA and UDP-GalNAc as donors were used, the enzyme sample obtained from cells co-expressing CSS1 and CSS2A achieved incorporation of the radiolabeled GlcUA into the acceptor substrate (Fig. 3), indicating the occurrence of polymerization for at least two saccharides. The same results were obtained when CSA-8 and CH-8 were used in place of CSC-8 (data not shown). In contrast, under the same assay conditions, the enzyme sample of coexpression of CSS1 and CSS2B did not show the incorporation of the radioactivity into the acceptor substrates (Fig. 3). These results suggest that the complex of CSS1 with CSS2A, but not with CSS2B, has chain polymerizing activity of CS.

We further identified CS initiating activity of these variants. The enzyme sample obtained from cells co-expressing CSS1 and CSS2/ChPF has been reported to exhibit both initiating and polymerizing activities using GlcAβ1–3Galβ1–3Galβ1–4Xylβ1-*O*-methoxyphenyl (14). In this experiment, when this acceptor was used, neither combination of CSS2A and CSS1 or CSS2B and CSS1 attained the incorporation (data not shown), suggesting that neither complex has CS initiating activity onto the linkage tetrasaccharide.

Localization of CSS2 Variants in the Cell—Glycosyltransferases involved in the biosynthesis of CS are supposed to be

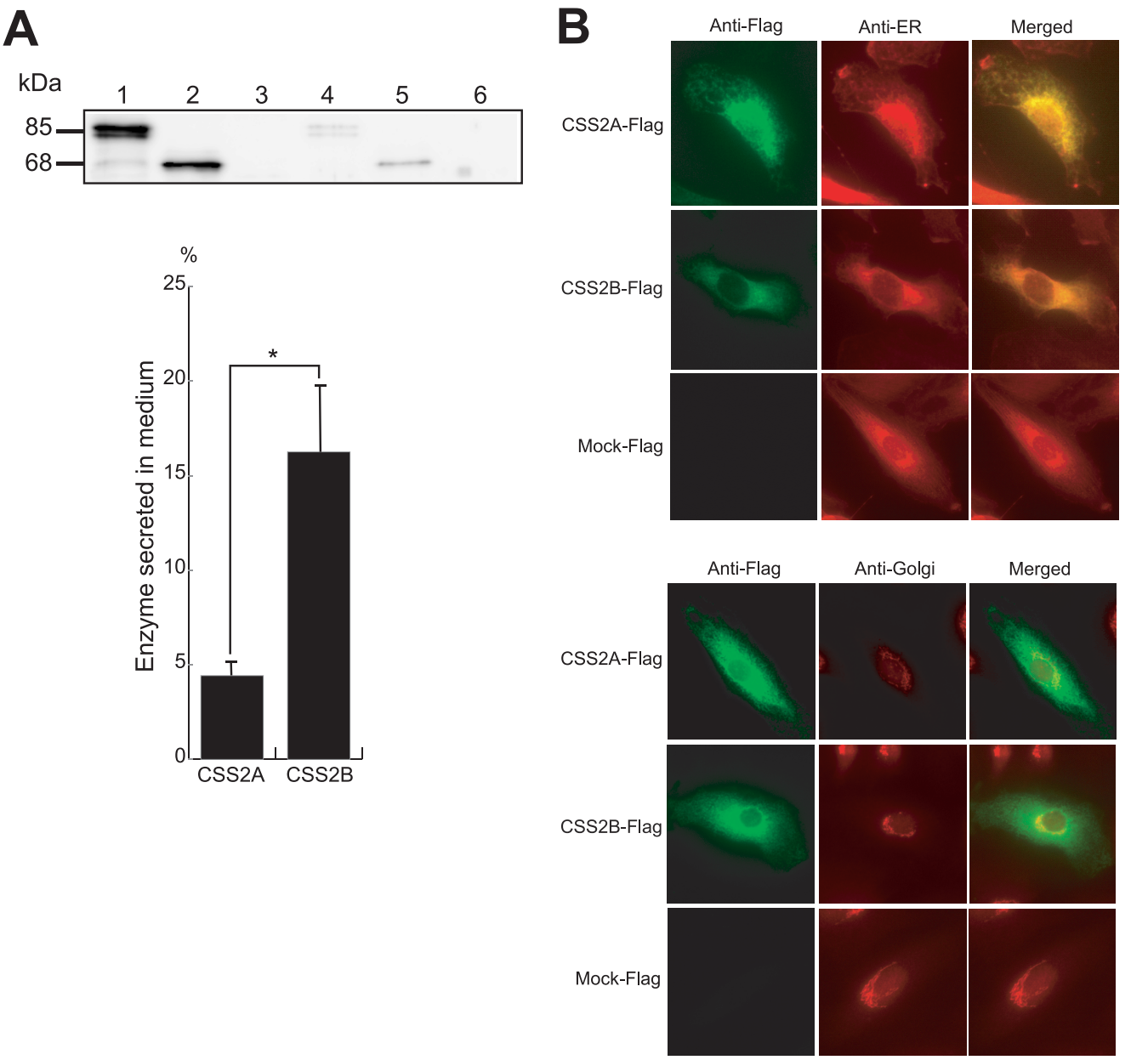

FIGURE 4. **Localization of the CSS2 variants.** *A*, the proportion of CSS2 variants in and out of cells is shown. Cell lysates and conditioned medium generated from cultured Balb 3T3 cells expressing CSS2A-FLAG and CSS2B-FLAG were subjected to Western blot analysis to evaluate the proportion of the CSS2 variants in and out of cells as described under "Experimental Procedures." *Lane 1*, CSS2A (cell lysate); *lane 2*, CSS2B (cell lysate); *lane 3*, mock (cell lysate); *lane 4*, CSS2A (medium); *lane 5*, CSS2B (medium); *lane 6*, mock (medium). The *lower panel* shows densitometric analysis of the CSS2 variants secreted into medium (data are expressed as the mean ± S.D., $n = 5$; *, $p < 0.001$; *t* test). Note that ~86% of CSS2B without a transmembrane domain remains in the cell although the proportion of CSS2B secreted in the medium is significantly higher than that of CSS2A. *B*, subcellular localization of CSS2 variants is shown. Cells overexpressing CSS2A-FLAG or CSS2B-FLAG were immunostained for FLAG, the ER, and the Golgi apparatus and observed using a fluorescence microscope as described under "Experimental Procedures." The *merged images* show the localization of CSS2A and CSS2B on both the ER and the Golgi apparatus.

resident in the ER and the Golgi apparatus (15, 27). Indeed, human CSS2 is localized at the intracellular membrane system (15). Because CSS2B lacks the N-terminal transmembrane domain, it may be secreted rapidly and may not contribute to CS biosynthesis. To investigate this, we expressed CSS2 variants whose C-terminal region of three amino acid residues were replaced with FLAG tag in COS-7 cells and measured their levels remaining in the cells and those secreted into the conditioned media. Western blot analysis after absorption with anti-FLAG M2-agarose gel demonstrated that more than 95% of CSS2A remained in the cells. Interestingly, more than 80% of CSS2B without the transmembrane domain were also found in the cells (Fig. 4*A*).

To further determine the intracellular localization of CSS2 variants, we expressed the FLAG-tagged CSS2 variants in the Balb 3T3 cells and performed immunohistochemical analysis. Double staining with either of the ER or the Golgi apparatus marker clearly demonstrated that both CSS2A and CSS2B were localized in both the ER and the Golgi apparatus (Fig. 4*B*). These observations suggest that CSS2B, lacking the transmem-

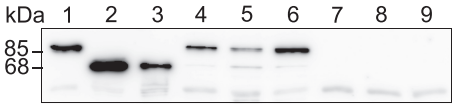

FIGURE 5. **Pulldown assays of co-expressed CSS2A, CSS2B, and CSS1 in various combinations.** Lysates of cells co-expressing two of CSS2A, CSS2B, and CSS1 in various combinations were pulled down with anti-FLAG M2-agarose gel. The gel slurry was subjected to Western blot analysis using anti-Myc antibody as a primary antibody as described under "Experimental Procedures." *Lane 1*, CSS2A-FLAG and CSS2A-Myc; *lane 2*, CSS2A-FLAG and CSS2B-Myc; *lane 3*, CSS2B-FLAG and CSS2B-Myc; *lane 4*, CSS2A-FLAG and CSS1-Myc; *lane 5*, CSS2B-FLAG and CSS1-Myc; *lane 6*, CSS1-FLAG and CSS1-Myc; *lane 7*, FLAG-AgMut-13 and CSS2A-Myc; *lane 8*, FLAG-AgMut-13 and CSS2B-Myc; *lane 9*, FLAG-AgMut-13 and CSS1-Myc.

brane domain, may bind to other molecules anchored onto the ER and the Golgi apparatus.

Homogeneous and Heterogeneous Interactions between CSS2 Variants and CSS1—A previous study reported that any two of either human CSS1, CSS2, CSS3, or chondroitin sulfate glucuronyltransferase interacted with each other to form a complex (15). To determine the partner of CSS2B, we carried out the pulldown assay using various combinations of CSS2A, CSS2B, and CSS1. For this analysis, FLAG- and Myc-tagged CSS1 and CSS2 variants (CSS1-FLAG, CSS2A-FLAG, CSS2B-FLAG, CSS1-Myc, CSS2A-Myc, and CSS2B-Myc) were generated, FLAG- and Myc-tagged enzymes were co-expressed in COS-7 cells, and the cell lysates were treated with anti-FLAG M2-agarose gel, which were then subjected to Western blot analysis using an anti-Myc antibody. A band at a molecular mass of 85 kDa corresponding to CSS2A-Myc was detected for the co-expression of CSS2A-FLAG and CSS2A-Myc (Fig. 5, *lane 1*). A 68-kDa band corresponding to CSS2B-Myc was detected for the co-expression of CSS2A-FLAG and CSS2B-Myc (Fig. 5, *lane 2*) and for that of CSS2B-FLAG and CSS2B-Myc (Fig. 5, *lane 3*). A 91-kDa band corresponding to CSS1-Myc was observed for the co-expression of CSS2A-FLAG and CSS1-Myc (Fig. 5, *lane 4*), CSS2B-FLAG and CSS1-Myc (Fig. 5, *lane 5*), and CSS1-FLAG and CSS1-Myc (Fig. 5, *lane 6*). No band was detected for the co-expression of FLAG-AgMut-13 with either CSS2A-Myc (Fig. 5, *lane 7*), CSS2B-Myc (Fig. 5, *lane 8*), or CSS1-Myc (Fig. 5, *lane 9*), confirming their specific interactions. These results suggest that CSS1, CSS2A, and CSS2B interact with each other homogeneously and heterogeneously and further suggest the presence of a multimolecular complex composed of two or more CS synthase family members rather than simple heterodimers.

To confirm the presence of a multimolecular complex, we carried out size exclusion chromatography and subsequent Western blot analysis using CSS2A-FLAG, CSS2B-FLAG, and CSS1-Myc in some combination. We observed a band at a molecular mass of 85 kDa corresponding to CSS2A at a highest density in the fraction 8 of the sample overexpressed with CSS2A-FLAG (supplemental Fig. S2*a*), two bands of 85 and 68 kDa corresponding to CSS2A and CSS2B, respectively, in fraction 8 of the sample co-expressed with CSS2A-FLAG and CSS2B-FLAG (supplemental Fig. S2*b*), and a band of 91 kDa corresponding to CSS1 for the fraction 8 of the sample co-expressed with CSS2A-FLAG, CSS2B-FLAG, and CSS1-Myc (supplemental Fig. S2*d*). In contrast, we detected faint bands in the fraction 14 (200~400 kDa) and 16 (50~100 kDa) in all the samples. These results indicate the presence of a huge complex composed of CS synthase family members.

CSS2B Inhibits CS Biosynthesis—The different ratios of expression of CSS2 variants in various tissues suggested distinct functions for CSS2B. As the major difference of the variants was that CSS2B exhibits substantially lower GlcAT activity than CSS2A and has no polymerizing activity when co-expressed with CSS1, we examined the levels of CS biosynthesis in COS-7 cells overexpressing either variant. Twenty-four hours after transfection of expression plasmid of either variant, CS was metabolically labeled with [^{35}S]sulfate for 24 h, as described under "Experimental Procedures." The cells overexpressing CSS2A showed up to a ~1.71-fold increase in CS levels in the cell lysates compared with the mock-transfected cells. In contrast, the cells overexpressing CSS2B showed ~50% CS levels that of the mock-transfected cells (Fig. 6*A*). Then we isolated GAG fractions labeled with [^{35}S]sulfate, treated it with a heparitinase mixture, and then applied it to gel chromatography to investigate CS chain length. The elution profiles showed three peaks for the sample of CSS2A-overexpressing cells, whereas those in mock-transfected cells showed two peaks (Fig. 6*B*). The peak shift for the largest molecular mass in CSS2A-overexpressing cells (Fig. 6*B*, *solid arrowhead*) as compared with mock-transfectant (Fig. 6*B*, *open arrowhead*), clearly indicated that CSS2A contributes to CS chain polymerization. In contrast, CS chains in CSS2B-overexpressing cells had only one peak (Fig. 6*B*, *short arrow*), which corresponded to the smallest molecular mass in both CSS2A-overexpressing cells and the mock-transfectant, suggesting that CSS2B inhibits the chain polymerization. We further confirmed that the peaks from CSS2A-overexpressing cells represent CS by gel chromatography of the sample pretreated with chondroitinase ABC. The elution profile showed two peaks, corresponding to disaccharide (Fig. 6*C*, *solid arrowhead*) and hexasaccharide (Fig. 6*C*, *open arrowhead*), suggesting that chondroitinase ABC-digested products of metabolically labeled CSs were disaccharide, GlcAβ1–3GalNAcβ1, and the hexasaccharide, GlcAβ1–3GalNAcβ1-GlcAβ1–3Galβ1–3Galβ1–4Xyl, respectively. The peaks for mock-transfectant and CSS2B-overexpressing cells similarly shifted into the two peaks by chondroitinase ABC digestion (data not shown).

Ratio of CSS2 Variants Correlates with Age-dependent Change of CS Chain Length in Brain of Mice—To address biological relevance of CSS2B, we examined the relationship of the expression level of CSS variants and CS chain length in brain. By real-time RT-PCR, the ratio of transcription levels of CSS2B to CSS2A was 0.10, 0.25, and 0.31 at newborn, 3 weeks, and 9 weeks, respectively (Fig. 7*A*), indicating an age-dependent increase in the ratio of CSS2B/CSS2A. In parallel, we isolated CS from brain labeled with sodium [^{3}H]borohydride and applied it to gel chromatography. The elution profile showed that the peak shifted to a smaller molecular mass with an increase in age (Fig. 7*B*). These results indicate a good *in vivo* correlation between shortening of CS chain length and an increase in the ratio of CSS2B to CSS2A during growth and suggest involvement of CSS2B in regulation of CS chain length.

Homology Modeling of CSS2 Variants—To obtain insight into the different functions of CSS2A and CSS2B on CS biosyn-

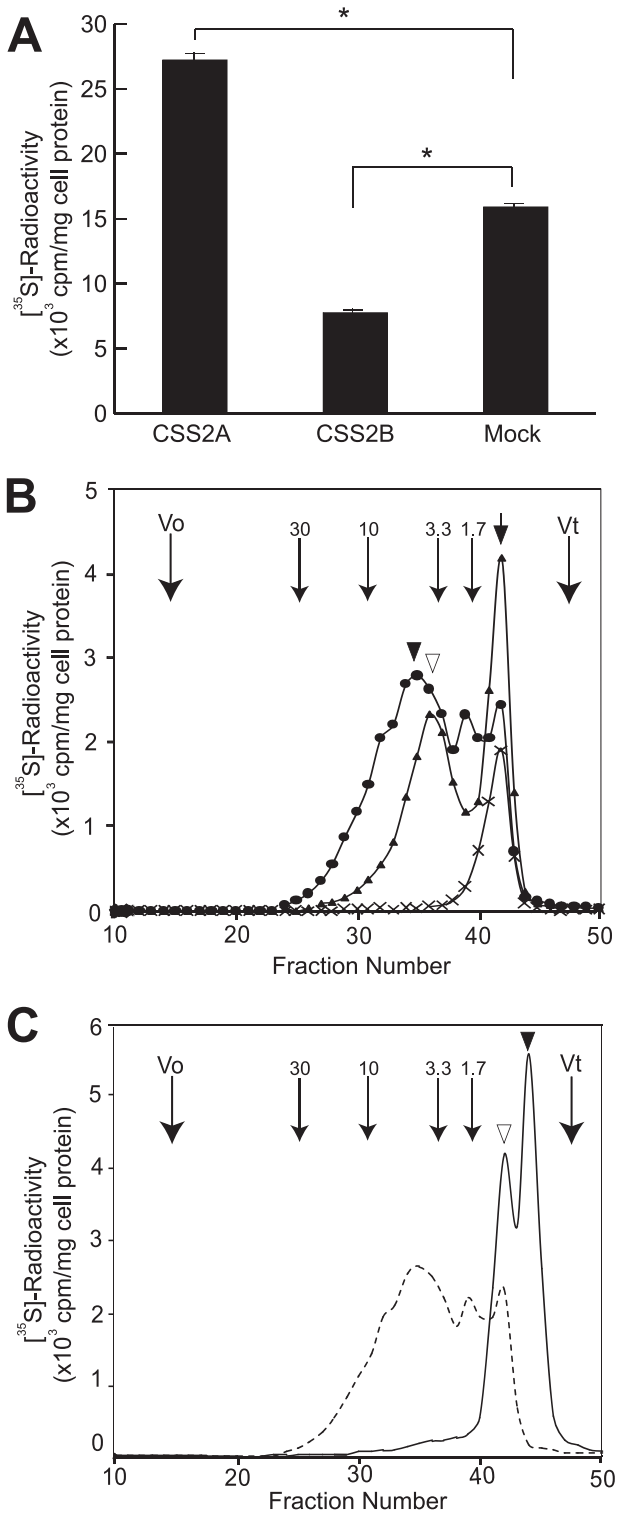

FIGURE 6. **Analysis of CS chains in COS-7 cells overexpressing CSS2 variants.** *A*, [^{35}S]sulfate incorporation of mock-transfected COS-7 cells and CSS2A- and CSS2B-overexpressing cells. The cells were metabolically labeled with [^{35}S]sulfate for 24 h. CS, extracted as described under "Experimental Procedures," was subjected to scintillation counting. Note that CSS2A-overexpressing cells exhibit a ~1.71-fold increase in CS levels compared with the mock-transfected cells, whereas CSS2B-overexpressing cells show an ~50% CS levels of the mock-transfected cells. The radioactivity is shown as the mean ± S.D. ($n = 3$; *, $p < 0.0001$; *t* test). *B*, shown is a comparison of the chain length of CS in CSS2 variants-overexpressing cells. The samples from [^{35}S]sulfate-labeled mock-transfected cells and CSS2A- and CSS2B-overexpressing cells were applied to a Superose 6 column, and effluent fractions (0.5 ml each) were analyzed for radioactivity as described under "Experimental Procedures." The elution profiles of the samples obtained from CSS2A-overexpressing cells (●), CSS2B-overexpressing cells (×), and mock-transfectant (▲) are shown. Note the peak shift of the largest molecular mass in CSS2A-overexpressing cells (*solid arrowhead*) from the mock-transfectant (*open arrowhead*). In contrast, the elution profile of the sample from CSS2B-overexpressing cells exhibits only one peak for the smallest molecular mass (*short arrow*). *C*, confirmation of the peaks in Fig. 6-*B* as CS chains is shown. The sample obtained from CSS2A-overexpressing cells pretreated with chondroitinase ABC was applied to gel chromatography, and effluent fractions (0.5 ml each) were analyzed for radioactivity. Elution profiles show two peaks (*solid line*) by chondroitinase ABC digestion. The *solid arrowhead* indicates the labeled disaccharide, GlcAβ1–3GalNAcβ1, and the *open arrowhead* indicates the hexasaccharide, GlcAβ1–3GalNAcβ1-GlcAβ1–3Galβ1–3Galβ1–4Xyl, composed of tetrasaccharide linkage legions and the labeled disaccharide. The elution profile of the non-treated sample is shown for comparison (*broken line*). *Numbered arrowheads 1.7*, *3.3*, *10*, and *30* indicate the eluted positions of chondroitin polysaccharides of known sizes (molecular size: 1,700, 3,300, 10,000, and 30,000, respectively).

thesis, we performed molecular modeling of their N-terminal domain using Mfng as a template. Fig. 8*A* shows amino acid sequences aligned between the Mfng and N-terminal domains of CSS2 variants. When the homology modeling of N-CSS2A was performed, the model structure built by MOE program showed the highest Verify Score (96.53, expected high score = 97.12). When the homology modeling of N-CSS2B was performed, the model structure built by DS program showed the highest Verify Score (70.71, expected high score = 74.27). Without the manual alignment of the first β-strand region of N-CSS2B, the highest Verify Score of model structure was 70.15 from DS program. Therefore, the modification of the alignment increased the plausibility of the model structure of N-CSS2B.

Because N-CSS2A and N-CSS2B exhibit only ~10% amino acid identity to Mfng, we could not perform an atomic level prediction of the three-dimensional structures of N-CSS2A and N-CSS2B. However, the spatial positions of amino acid residues are expected to be accurate (28). When the shape of the protein surface that interacts with UDP-Mn^{2+} was compared between a complex of N-CSS2A-UDP-Mn^{2+} and that of N-CSS2B-UDP-Mn^{2+}, the surface of N-CSS2A (Fig. 8*B*) resembled that of Mfng (Fig. 8*C*), whereas the surface of N-CSS2B (Fig. 8*D*) was considerably different from that of Mfng. From the model structure of N-CSS2A-UDP-Mn^{2+} complex, Leu-124, Ser-126, Thr-129, Pro-205, Asp-206, Ala-207, Leu-316, and His-336 residues were estimated to be involved in the interaction of UDP-Mn^{2+}. Especially, Pro-205, Asp-206, and Ala-207 corresponded to the D*X*D motif in GT-A glycosyltransferase. For N-CSS2B, Ala-5, Leu-6, Arg-10, Pro-11, Pro-37, Ala-39, His-82, Arg-112, Leu-143, Pro-145, and His-163 were estimated to be involved in the interaction with UDP-Mn^{2+}, and Pro-37 and Ala-39 appeared to correspond to the D*X*D motif (Fig. 8*A*). When the amino acid residues expected to be involved in the interactions with phosphate group of UDP were compared, nearly the same amino acid residues were involved between CSS2A and CSS2B. In contrast, the amino acid residues involved in the interaction with the uridine group were different between the two. For instance, CSS2B lacks the amino acid residues Leu-124, Ser-126, and Thr-129, presumably involved in the interaction with the uridine group in CSS2A. Instead of these residues, Ala-5, Leu-6, Arg-10, and Pro-11 in CSS2B were

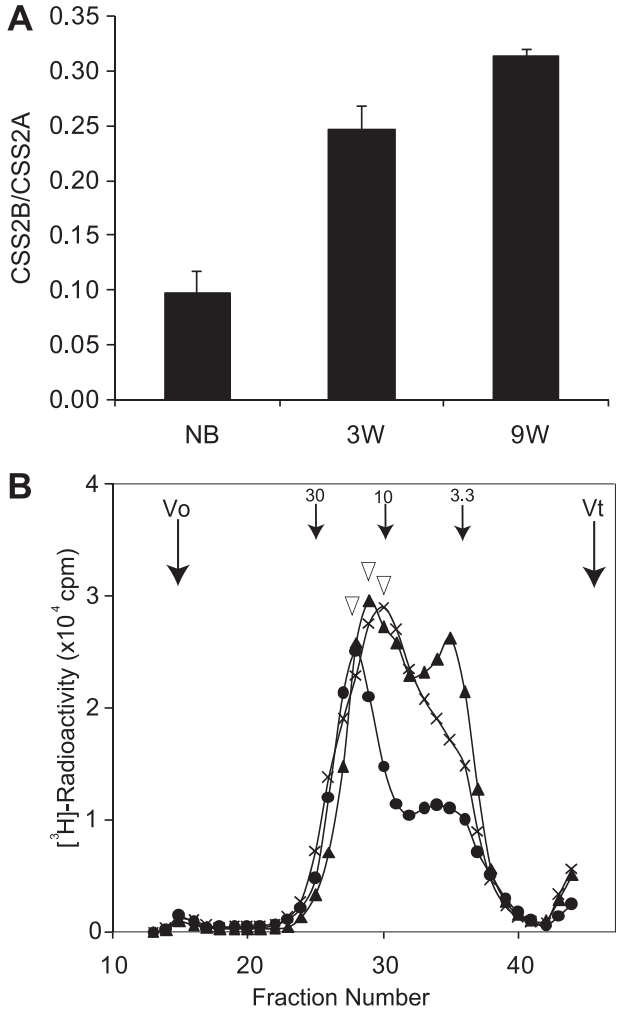

FIGURE 7. **Ratio of expression levels of CSS2B to CSS2A (*A*) and CS chain length (*B*).** *A*, the ratio of CSS2 variants in mice at newborn (*NB*), 3 weeks (*3W*), and 9 weeks (*9W*) was analyzed by real-time RT-PCR. The expression level of CSS2B was divided with that of CSS2A. Data are indicated as the mean ± S.D. ($n = 3$, at each age). Two identical experiments show the same results. *B*, CS was isolated from brain at newborn, 3 weeks, and 9 weeks, labeled with sodium [^{3}H]borohydride, and applied to a Superose 6 column. The effluent fractions (0.5 ml each) were analyzed for radioactivity, as described under "Experimental Procedures." The elution profiles of the samples obtained from brain at newborn (●), 3 weeks (▲), and 9 weeks (×) are shown. Note the peak of the largest molecular mass in each sample (*open arrowhead*) shifts to positions of smaller molecules with an increase in age. Two identical experiments ($n = 2$, at each age) showed the same elution profile. *Numbered arrows 3.3*, *10*, and *30* indicate molecular sizes 3,300, 10,000, and 30,000, respectively.

estimated to be involved in the interaction with the uridine group. Even if the conformation of the catalytic site of N-CSS2B is actually different from our model, large conformational modification of the uridine group-binding site induced by the absence of the N-terminal region of 162 amino acid residues is likely to cause the decrease in GlcAT activity in CSS2B.

DISCUSSION

In this study we have found cDNA for a splice variant of mouse CSS2/ChPF and have shown for the first time that both the original CSS2 and the splice variant, designated CSS2A and CSS2B, respectively, are synthesized as proteins. Compared with CSS2A, CSS2B lacks the N-terminal region of 162 amino acid residues including the N-terminal transmembrane domain and a putative *N*-linked oligosaccharide attachment site. Their characterization revealed several points as follows. 1) Whereas CSS2B exhibits a similar level of GalNAcT activity to that of CSS2A, it exhibits ~26% GlcAT activity that of CSS2A; 2) even without the N-terminal transmembrane domain, a large proportion of CSS2B remains in the cell; 3) CSS1 and CSS2 variants may form a multiple complex; 4) whereas co-expression of CSS1 and CSS2A achieves CS chain polymerization *in vitro*, that of CSS1 and CSS2B does not; 5) by metabolic labeling analysis, whereas CSS2A facilitates CS biosynthesis, CSS2B inhibits it. Taken together, these results postulate a regulatory mechanism of CS biosynthesis by two CSS2 variants with different functions.

As CSS2B is translated from the ATG-2 in the exon 2 of CSS2A, the β3-glycosyltransferase, β4-glycosyltransferase, and D*X*D motifs, critical for the catalytic function of CSS2A, are conserved in CSS2B. Although CSS2B exhibits the dual enzymatic activities of GalNAcT-II and GlcAT-II *in vitro*, its GlcAT activity is ~26% that of CSS2A. Homology modeling of the N-terminal domain of both variants strongly suggests that removal of the region, as observed in CSS2B, abrogates a putative UDP-sugar binding site in N-CSS2A model and generates another putative UDP-sugar binding site. Therefore, the decrease of GlcAT activity in CSS2B is likely due to lack of an N-terminal region of 162 amino acid residues. Our *in vitro* assay has revealed that, whereas CSS2A co-expressed with CSS1 achieves CS polymerization, CSS2B with CCS1 does not. This suggests that CS polymerization requires a certain level of GlcAT activity of CSS2, or alternatively, the structure of the complex including CSS1 and CSS2B is different from the functional complex including CSS1 and CSS2A.

It has been reported that any two of the CS glycosyltransferases (CSS1, CSS2, and CSS3) co-expressed in a cell form a complex and achieve polymerization; however, these enzymes, when individually expressed, do not exhibit polymerizing activity, suggesting that the formation of the functional enzyme complex requires any two of these enzymes in the cell (18). In this study a series of pulldown assays using co-expressed enzymes have revealed that any one of these enzymes pulled down another enzyme, consistent with the previous report (18). Moreover, we have observed that any of the CSS1 and CSS2 variants pulled down the same enzyme, implicating that these enzymes form the homogenous multimer. Our results suggest that individual enzymes do not have the specificity of partnership. As co-expression of two different enzymes is required for polymerization, there appears to be a mechanism by which different enzymes form a functional complex for efficient CS polymerization. Although our data do not eliminate the possibility that two different glycosyltransferases form a heterodimer rather non-specifically, they suggest that a functional complex for CS polymerization involves three or more molecules. Our results obtained by size exclusion chromatography support this, demonstrating CSS2 variants were eluted in fractions at substantially higher molecular mass (supplemental Fig. S2). Further studies remain to be performed to identify the other molecules that participate in formation of the functional complex of *in vivo* CS chain polymerization.

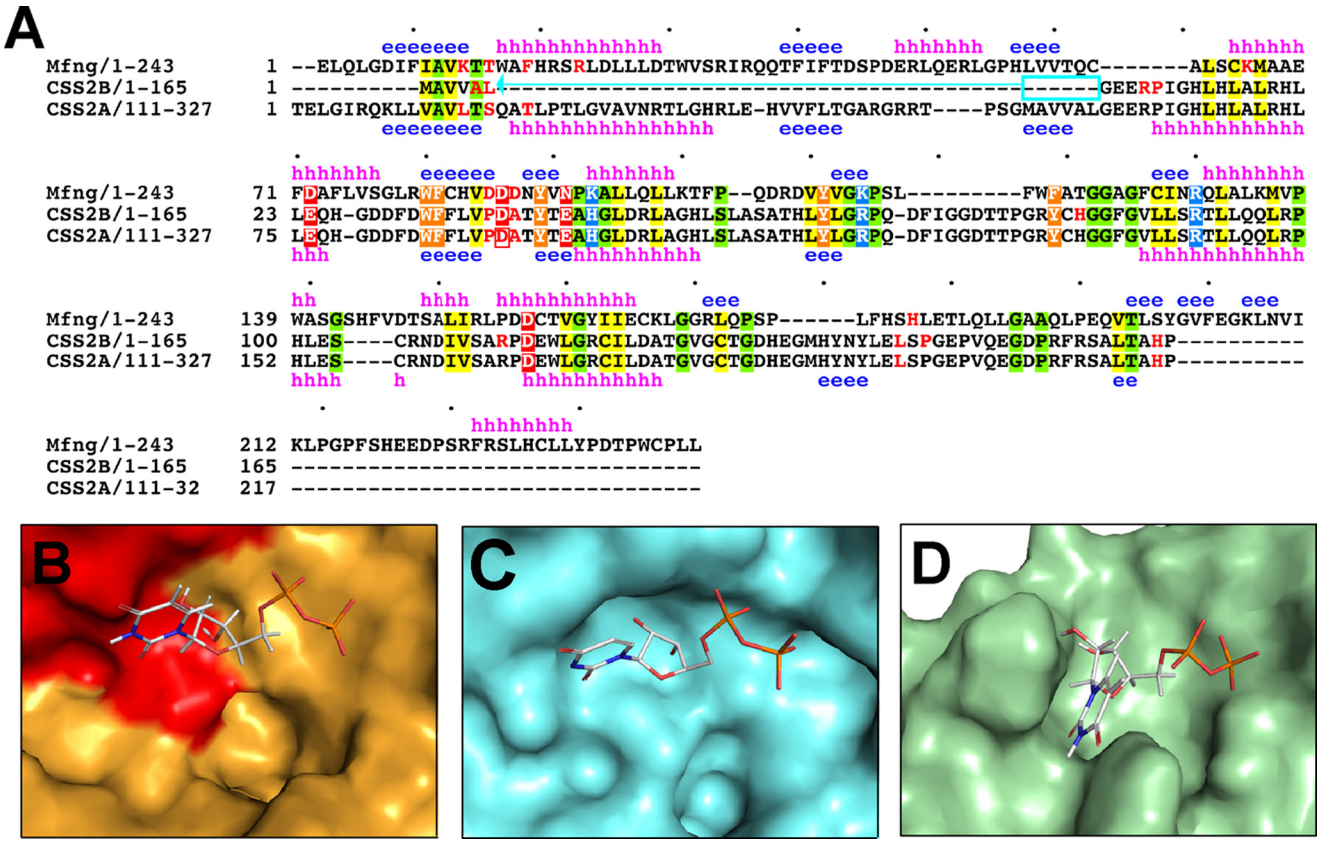

FIGURE 8. **Homology modeling of N-CSS2A and N-CSS2B.** *A*, alignment of Mfng, N-CSS2A, and N-CSS2B is shown. For modeling of N-CSS2B, the N-terminal region of six amino acid residues of CSS2B, which is expected to form a β-strand, is aligned to the N-terminal β-strand of Mfng. The actual secondary structure of Mfng and predicted secondary structure of N-CSS2A by Phyre is shown (*h*, α-helix; *e*, β-strand) *above* and *below* the amino acid sequence of Mfng and CSS2A, respectively. Amino acid residues identified to interact with UDP in Mfng and those speculated in N-CSS2A and N-CSS2B are colored in *red*. Background of amino acid residues is colored if amino acid residues with similar chemical properties are conserved in three sequences. *B*, shown is the presumptive molecular surface of N-CSS2A-UDP-Mn^{2+}. The region missing in N-CSS2B is colored in *red*. *C*, shown is the molecular surface of Mfng-UDP-Mn^{2+} (PDB code 2j0b). *D*, shown is the presumptive molecular surface of N-CSS2B-UDP-Mn^{2+}. The stick models in *B–D* indicate the UDP molecule. The pictures *B–D* are drawn by superimposing N-CSS2A and N-CSS2B to Mfng and are shown from the same viewpoint using PyMol.

Although CSS2B lacks the N-terminal transmembrane, its major proportion was localized in the cell, which is probably due to its interaction with other glycosyltransferases with an N-terminal transmembrane domain. Our immunocytochemical analysis has demonstrated that both CSS2 variants are localized in both the ER and the Golgi apparatus, which is consistent with previous reports (15). The presence of these variants in the ER is likely due to their overexpression in this system.

CS is polymerized in chain length varying from 20 to 50 kDa, depending on the core protein, tissue location, age, and disease conditions (29–32). Comparison of the CS chain length by different pairs of CSSs (18) suggested that the length is dependent on the pair of CSSs co-expressed and that the pair of CSS1 and CSS2 polymerizes CS chains most efficiently. Among CSSs, CSS3 is expressed at quite low levels compared with CSS1 and CSS2 (11, 21). Thus, it is likely that the pair of CSS1 and CSS2 plays the major role in CS chain polymerization. Our analysis of CS biosynthesis has clearly demonstrated substantial involvement of CSS2 in CS biosynthesis and has further demonstrated a distinct function of its variant, CSS2B. Overexpression of CSS2A facilitated CS biosynthesis, including chain polymerization in COS-7 cells (Fig. 6), indicating that the level of endogenous CSS2 is unsaturated in COS-7 cells and that overexpression of CSS2A increases the number of the functional complex of CS polymerization. In contrast, overexpression of CSS2B substantially inhibited endogenous CS biosynthesis, suggesting that CSS2B disturbs formation of the functional complex by competing with CSS2A. The opposite function of CSS2 variants suggests that CSS2 regulates CS chain polymerization by balancing the ratio of the variants.

Molecular modeling predicted that CSS2B is structurally stable but CSS2B lacks an *N*-glycosylation site and a cysteine. Actually, we have detected not only the original CSS2A but also CSS2B variant as endogenous proteins. To date, chondroitin-4-sulfotransferase 1 (20) and a disease condition like arthritis (33) are reported to affect the CS chain length as well as CS glycosyltransferases. Our observation that CS chains in brain become shorter during growth, concomitant with an increase in the ratio of CSS2B expression, suggests the biological relevance of CSS2B and presents another member participating in the regulation of CS chain length. Interestingly, the ratio of CSS2 variants expressed is different among tissues. Whereas MEFs express more than 95% of CSS2A, brain at 9 weeks expresses ~75 and 25% of CSS2A and CSS2B, respectively. As CS chain length is known to vary among tissues, the ratio of CSS2 variants may be involved in the regulation of the length.

It has not been determined whether CSS2 variants are present in other species, including humans. So far, no human cDNA

comparable with mouse CSS2B has been identified. As shown in Fig. 1, CSS2B has an additional exon 1′ in intron 1. The human genomic locus of CSS2 contains a putative exon corresponding to mouse exon 1′, exhibiting 76% nucleotide sequence identity. This region has a consensus GT-AG splice sequence and some exonic splicing enhancer sequences. These data strongly suggest the presence of exon 1′ in humans. The putative exon 1′ of the human CSS2 genome contains ATG, and if translation initiates at this ATG, a longer variant with a N-terminal region of 55 amino acid residues different from the putative human CSS2B would be synthesized. Although the human database has no information showing transcription of the putative exon 1′, the Ensembl database (34) shows that the mRNA sequence that encodes CSS2A exhibits another translation initiation site that may synthesize CSS2B in mouse (Ensembl gene accession no. OTTMUS600000019412). Similarly, the mRNA of human CSS2 may be used for the synthesis of CSS2B as well as CSS2A.

Our study proposes a mechanism of regulation of CS biosynthesis by CSS2 variants. Characterization of CS glycosyltransferases should involve their splice variants because they may exhibit distinct functions. Systematic analysis using recombinant enzymes, deduced by cDNAs showing putative variants, will lead to determination of the enzyme complex and elucidation of the mechanisms of CS biosynthesis. In addition, our findings implicate that CSS2B may serve as a useful tool for regulation of CS biosynthesis. As inhibition of expression of a glycosyltransferase may not suppress CS biosynthesis due to compensation by other CSSs, overexpression of CSS2B may be applied as an alternative method to suppression of CS biosynthesis.

REFERENCES

1. Kjellén, L., and Lindahl, U. (1991) *Annu. Rev. Biochem.* **60,** 443–475
2. Esko, J. D., and Selleck, S. B. (2002) *Annu. Rev. Biochem.* **71,** 435–471
3. Prydz, K., and Dalen, K. T. (2000) *J. Cell. Sci.* **113,** 193–205
4. Sugahara, K., and Kitagawa, H. (2000) *Curr. Opin. Struct. Biol.* **10,** 518–527
5. Perrimon, N., and Bernfield, M. (2000) *Nature* **404,** 725–728
6. Sugahara, K., Mikami, T., Uyama, T., Mizuguchi, S., Nomura, K., and Kitagawa, H. (2003) *Curr. Opin. Struct. Biol.* **13,** 612–620
7. Deepa, S. S., Yamada, S., Zako, M., Goldberger, O., and Sugahara, K. (2004) *J. Biol. Chem.* **279,** 37368–37376
8. Bao, X., Muramatsu, T., and Sugahara, K. (2005) *J. Biol. Chem.* **280,** 35318–35328
9. Oohira, A., Matsui, F., Tokita, Y., Yamauchi, S., and Aono, S. (2000) *Arch. Biochem. Biophys.* **374,** 24–34
10. Morgenstern, D. A., Asher, R. A., and Fawcett, J. W. (2002) *Prog. Brain Res.* **137,** 313–332
11. Yada, T., Gotoh, M., Sato, T., Shionyu, M., Go, M., Kaseyama, H., Iwasaki, H., Kikuchi, N., Kwon, Y. D., Togayachi, A., Kudo, T., Watanabe, H., Narimatsu, H., and Kimata, K. (2003) *J. Biol. Chem.* **278,** 30235–30247
12. Gotoh, M., Yada, T., Sato, T., Akashima, T., Iwasaki, H., Mochizuki, H., Inaba, N., Togayachi, A., Kudo, T., Watanabe, H., Kimata, K., and Narimatsu, H. (2002) *J. Biol. Chem.* **277,** 38179–38188
13. Kitagawa, H., Uyama, T., and Sugahara, K. (2001) *J. Biol. Chem.* **276,** 38721–38726
14. Kitagawa, H., Izumikawa, T., Uyama, T., and Sugahara, K. (2003) *J. Biol. Chem.* **278,** 23666–23671
15. Izumikawa, T., Koike, T., Shiozawa, S., Sugahara, K., Tamura, J., and Kitagawa, H. (2008) *J. Biol. Chem.* **283,** 11396–11406
16. Sato, T., Gotoh, M., Kiyohara, K., Akashima, T., Iwasaki, H., Kameyama, A., Mochizuki, H., Yada, T., Inaba, N., Togayachi, A., Kudo, T., Asada, M., Watanabe, H., Imamura, T., Kimata, K., and Narimatsu, H. (2003) *J. Biol. Chem.* **278,** 3063–3071
17. Uyama, T., Kitagawa, H., Tanaka, J., Tamura, J., Ogawa, T., and Sugahara, K. (2003) *J. Biol. Chem.* **278,** 3072–3078
18. Izumikawa, T., Uyama, T., Okuura, Y., Sugahara, K., and Kitagawa, H. (2007) *Biochem. J.* **403,** 545–552
19. Uyama, T., Ishida, M., Izumikawa, T., Trybala, E., Tufaro, F., Bergström, T., Sugahara, K., and Kitagawa, H. (2006) *J. Biol. Chem.* **281,** 38668–38674
20. Klüppel, M., Wight, T. N., Chan, C., Hinek, A., and Wrana, J. L. (2005) *Development* **132,** 3989–4003
21. Yada, T., Sato, T., Kaseyama, H., Gotoh, M., Iwasaki, H., Kikuchi, N., Kwon, Y. D., Togayachi, A., Kudo, T., Watanabe, H., Narimatsu, H., and Kimata, K. (2003) *J. Biol. Chem.* **278,** 39711–39725
22. Sugiura, N., Baba, Y., Kawaguchi, Y., Iwatani, T., Suzuki, K., Kusakabe, T., Yamagishi, K., Kimata, K., Kakuta, Y., and Watanabe, H. (2010) *J. Biol. Chem.* **285,** 1597–1606
23. Sasai, K., Ikeda, Y., Tsuda, T., Ihara, H., Korekane, H., Shiota, K., and Taniguchi, N. (2001) *J. Biol. Chem.* **276,** 759–765
24. Kelley, L. A., and Sternberg, M. J. (2009) *Nat. Protoc.* **4,** 363–371
25. Jinek, M., Chen, Y. W., Clausen, H., Cohen, S. M., and Conti, E. (2006) *Nat. Struct. Mol. Biol.* **13,** 945–946
26. Suzuki, N., Toyoda, H., Sano, M., and Nishiwaki, K. (2006) *Dev. Biol.* **300,** 635–646
27. Paulson, J. C., Weinstein, J., and Schauer, A. (1989) *J. Biol. Chem.* **264,** 10931–10934
28. Martí-Renom, M. A., Stuart, A. C., Fiser, A., Sánchez, R., Melo, F., and Sali, A. (2000) *Annu. Rev. Biophys. Biomol. Struct.* **29,** 291–325
29. Maeda, N., Fukazawa, N., and Hata, T. (2006) *J. Biol. Chem.* **281,** 4894–4902
30. Brown, M. P., Trumble, T. N., Plaas, A. H., Sandy, J. D., Romano, M., Hernandez, J., and Merritt, K. A. (2007) *Osteoarthritis Cartilage* **15,** 1318–1325
31. Roughley, P. J., and White, R. J. (1980) *J. Biol. Chem.* **255,** 217–224
32. Mitchell, D., and Hardingham, T. (1982) *Biochem. J.* **202,** 387–395
33. Bollet, A. J., and Nance, J. L. (1966) *J. Clin. Invest.* **45,** 1170–1177
34. Hubbard, T. J., Aken, B. L., Ayling, S., Ballester, B., Beal, K., Bragin, E., Brent, S., Chen, Y., Clapham, P., Clarke, L., Coates, G., Fairley, S., Fitzgerald, S., Fernandez-Banet, J., Gordon, L., Graf, S., Haider, S., Hammond, M., Holland, R., Howe, K., Jenkinson, A., Johnson, N., Kahari, A., Keefe, D., Keenan, S., Kinsella, R., Kokocinski, F., Kulesha, E., Lawson, D., Longden, I., Megy, K., Meidl, P., Overduin, B., Parker, A., Pritchard, B., Rios, D., Schuster, M., Slater, G., Smedley, D., Spooner, W., Spudich, G., Trevanion, S., Vilella, A., Vogel, J., White, S., Wilder, S., Zadissa, A., Birney, E., Cunningham, F., Curwen, V., Durbin, R., Fernandez-Suarez, X. M., Herrero, J., Kasprzyk, A., Proctor, G., Smith, J., Searle, S., and Flicek, P. (2009) *Nucleic Acids Res.* **37,** D690–D697
35. Shi, J., Blundell, T. L., and Mizuguchi, T. (2001) *J. Mol. Biol.* **310,** 243–257
36. Tomii, K., and Akiyama, Y. (2004) *Bioinformatics* **20,** 594–595
37. Jones, D. T. (1999) *J. Mol. Biol.* **287,** 797–815